

PAPER • OPEN ACCESS

Optical properties of $\text{Si}_x\text{Ti}_y\text{C}_z\text{O}_w$ composite nanopowder obtained by pulsed plasma chemical method

To cite this article: G Kholodnaya *et al* 2018 *J. Phys.: Conf. Ser.* **1115** 022029

View the [article online](#) for updates and enhancements.

You may also like

- [Isovalent Co-Substitution of Iron and Titanium into Single-Crystal NMC622](#)
Macgregor F. Macintosh, Mohsen Shakouri and M. N. Obrovac
- [Temperature Dependent Dielectric and Structural Properties of \$\(\text{Ba}_{1-x}\text{Ca}_x\)\(\text{Zr}_{0.4}\text{Ti}_{0.6}\)\text{O}_3\$ \(0.140 x 0.160\) Ceramics](#)
Don Biswas, Prolay Sharma and N. S. Panwar
- [Initiation of Organized Nanopore/Nanotube Arrays in Anodized Titanium Oxide: I. Criterion for Initiation](#)
Que AnhS. Nguyen, Yash V. Bhargava and Thomas M. Devine



The Electrochemical Society
Advancing solid state & electrochemical science & technology



249th
ECS Meeting
May 24-28, 2026
Seattle, WA, US
Washington State
Convention Center

Spotlight Your Science

**Submission deadline:
December 5, 2025**

SUBMIT YOUR ABSTRACT

Optical properties of $\text{Si}_x\text{Ti}_y\text{C}_z\text{O}_w$ composite nanopowder obtained by pulsed plasma chemical method

G Kholodnaya¹, F Konusov¹, R Sazonov¹, D Ponomarev¹ and M Kaikanov²

¹National Research Tomsk Polytechnic University, 30 Lenin Ave., 634050, Tomsk, Russia

²Nazarbayev University, 53 Kabanbay batyr ave., Astana, 010000, Kazakhstan

E-mail: galina_holodnaya@mail.ru

Abstract. This paper presents the results of an experimental investigation on the optical properties of the $\text{Si}_x\text{Ti}_y\text{C}_z\text{O}_w$ nanopowders, produced by the pulsed plasma chemical method. Pulsed plasma chemical synthesis is realized on the laboratory stand, including a plasma chemical reactor (6 l) and TEA-500 electron accelerator. The parameters of the electron beam are as follows: 400-450 keV electron energy, 60 ns half-amplitude pulse duration, up to 200 J pulse energy, and 5 cm beam diameter. The spectrum of the diffuse reflection coefficient $R(h\nu)$ was measured using the AvaSpec-2048-2 (Avantes) spectrometer with the AvaLight-DHS light source (deuterium and halogen-tungsten lamp) and an integrating sphere. The band gap of the obtained composite is 2.03–3.12 eV.

1. Introduction

Because of some useful properties, nanocomposites of the various types have found wide application in the various fields of industry (electronics, electrical engineering, etc.). Composite materials which consist of organic and metal nanocomponents ($\text{TiO}_2\text{-C}$, $\text{SiO}_2\text{-C}$) are especially in demand in microelectronics, optics, as oxidation catalysts for chemical and petrochemical production processes [1-14]. They have high sensitivity to light and catalytic activity. In particular, the $\text{SiO}_2\text{-C}$ nanocomposite is used to fabricate an electrode with a high specific capacity on lithium-ion batteries [3]. Composites which contain titanium oxide are good photocatalysts [4]. At present, the $\text{SiO}_2\text{/C}$ nanocomposite is obtained by the various methods: chemical [5], sol-gel method [6], electroforming and thermal treatment [7], and pyrolysis [8].

In [9], the hollow SiO_2 nanospheres were obtained using a modified Stöber method. The hollow composite Si-SiC nanospheres were first obtained by the reduction of the hollow SiO_2 nanospheres using the method of magnetothermal reduction at low temperature. The SiO_2 nanospheres and Si-SiC composite nanospheres with a hollow structure were studied using scanning electron microscopy and transmission electron microscopy. Absorption-desorption measurement showed that the Si-SiC composite nanospheres had a large BET surface area of 150.33 m^2/g and a pore volume of about 12.9 nm³; in addition, the hollow structure was indirectly confirmed. X-ray diffraction, X-ray photoelectron spectroscopy, and thermogravimetric analysis were also performed to characterize the microstructure and composition of the final samples.

In [10], the $\text{SiO}_2\text{/C}$ composite was prepared on the basis of phenolic resins. A composite material was obtained with two different structures, one of silicon dioxide and the other of carbon. These



structures were independent. The physical and chemical properties of the composite were studied. The SiO₂/C nanocomposites have a narrow pore size distribution in the mesoporous region. In [11], the SiO₂/C composites were synthesized in one stage of the process by oxidizing hexamethyldisiloxane vapors in the C₂H₂ atmosphere with oxygen. The synthesized composites with high carbon content were obtained. The carbon content can be adjusted from 1.4 to 14 mass %, thereby the specific surface area varies from 31 to 121 m²/g. It is shown that regardless of the composition, the synthesized particles consist of the nanoclusters of silicon oxide and carbon and form a homogeneous structure of the nanocomposite. The thermal treatment of the powders at 1400 to 1500°C in an argon atmosphere resulted in the formation of fibrous β-SiC/SiO₂ composites. The number of nanofibers depends on the fraction of carbon in the original SiO₂-C powder.

The TiO₂/C composites are also currently produced mainly using a sol-gel method [15-20]. In [15], titanium dioxide particles encapsulated with carbon (graphene) were obtained. The samples have the crystal structure of anatase. The average particle size of the titanium dioxide ranged between 15 and 20 nm. When encapsulated, the formation of two types of particles was observed in TEM images, while the authors noted that the titanium dioxide particles were located in a carbon capsule. The sizes of particles and carbon-containing capsules ranged from 150 to 200 and from 700 to 1000 nm, respectively. The results of investigations showed in [16] that to increase the photocatalytic activity of the TiO₂/C composite it is necessary to increase the pyrolysis temperature (above 600°C).

The authors [17] believe that the best photocatalytic activity among the samples under consideration belongs to the sample, which contains 96% of rutile and 4% of anatase. It is known that due to the denser packing of ions in the rutile crystal, their mutual attraction increases, while photochemical activity decreases. The authors indicate that the presence of the carbon phase plays an important role in the photo catalysis mechanism for the synthesized samples. However, the authors point out the need for additional studies to fully understand the cause of an increase in the photocatalytic activity of the synthesized samples having rutile as predominantly crystalline lattice.

The TiO₂/C composite was obtained using a hydrothermal method in [21]. The presence of carbon in the composites results in the enhanced photocatalytic activity. Moreover, additional calcination of the samples has a positive effect on the photocatalytic activity. In [22], titanium dioxide and composites on its base were obtained using the hydrothermal method. Titanium dioxide was obtained from Ti(OCH(CH₃)₂)₄. To prepare this composite, 2,3-dihydroxynaphthalene was used as a carbon precursor. The synthesized composites mainly consist of rutile (>90%), while anatase content is about 10%. The photocatalytic activity of the samples was evaluated by the time of the decomposition of water into oxygen and hydrogen. The paper presents the data only on hydrogen. The experiment was carried out under the solar irradiation of the synthesized oxides and water. The photocatalytic decomposition of H₂O does not occur when titanium dioxide is used as a catalyst, even after 10 hours of irradiation. Doubling the C content increased the amount of decomposed hydrogen. In that case, carbon acted as an electron acceptor, which minimized electron-hole recombination, and, as a consequence, increased photocatalytic activity.

In [23], the authors obtained three composites: TiO₂/activated carbon (AC), TiO₂/carbon (C), and TiO₂/polyaniline (PANi). The latter composite was obtained during pyrolysis. The TiO₂/activated carbon (TiO₂/AC) sample was obtained after treatment of TiO₂/carbon in the KOH solution, followed by ignition at a temperature of 4500°C. The photocatalytic performance for the degradation of methylene blue was evaluated under UV light irradiation. The conversion ratio of methylene blue under UV light irradiation with 98>84.7>69% is for TiO₂/AC>TiO₂/C>TiO₂/PANi, respectively.

The results of theoretical studies (the mechanism of photo oxidation of CH₃OH with the TiO₂/C composite) are presented in [33]. The authors of many works associate an increase in photocatalytic activity with the peculiarity of the introduction of carbon on the surface of titanium dioxide, while indicating that oxygen is replaced by carbon during doping. The introduction of carbon is due to the electrons of the conduction band and localized holes, whose energy is within the forbidden band.

This paper presents the results of a study of the synthesis of the Si_xTi_yC_zO_w composite by a pulsed plasma chemical method. The useful properties of TiO₂ – catalytic activity, high reflectivity, etc. – can

be significantly enhanced by changing the structure of titanium dioxide in the presence of amorphous silicon dioxide. Using a cheap carrier for titanium dioxide can significantly reduce the cost of the synthesized material while maintaining its useful qualities. The $\text{Si}_x\text{Ti}_y\text{C}_z\text{O}_w$ composite material is also of interest regarding metallographic studies of changes in the structure of crystalline titanium dioxide when embedded in an amorphous silicon dioxide and carbon matrix.

2. Experimental setup

The $\text{Si}_x\text{Ti}_y\text{C}_z\text{O}_w$ composite were obtained using a pulsed plasma chemical method. This method of synthesis is based on the bulk excitation of the reaction gas by a pulsed electron beam and organization of the reaction process over the whole excitation region.

The energy expenses of the beam are significantly lower than the energy of the chemical endothermal synthesis reactions. Hence, the potentially high performance is reached in the practical realization of the method. Using plasma generated by the pulsed electron beam during synthesis enables to decrease unproductive energy losses, to vary the properties (size of the particles, crystal lattice) of the final product, to make the process more technological and easy-to-control. Figure 1 presents the scheme for obtaining the $\text{Si}_x\text{Ti}_y\text{C}_z\text{O}_w$ composite.

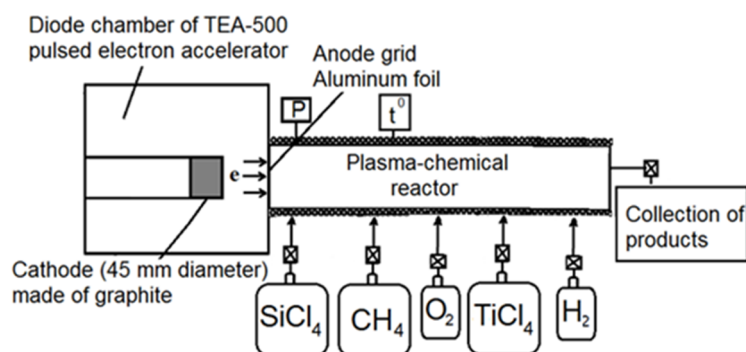


Figure 1. Schematic of experimental set-up.

The $\text{Si}_x\text{Ti}_y\text{C}_z\text{O}_w$ composite was synthesized in two consecutive stages. In the first stage, a carbon-containing composite based on silicon oxide was produced. For this, silicon tetrachloride, methane and oxygen were introduced into the plasma chemical reactor. The electron beam was injected into the mixture. It initiated a combustion reaction of methane, which was accompanied by the release of a significant amount of energy and the formation of radicals, as well as the dissociation of silicon tetrachloride with the formation of atomic chlorine. Afterwards, titanium tetrachloride, oxygen and hydrogen were introduced into the plasma chemical reactor. The plasma-chemical reactor was heated for 10 minutes at a temperature of about 65°C . Then the electron beam was injected into the reactor. It initiated a hydrogen burning reaction, which was accompanied by the release of a significant amount of energy and the formation of radicals, as well as the dissociation of titanium tetrachloride with the formation of atomic chlorine (which entered into an exothermic reaction with hydrogen). Two batches of the composite were produced (1 sample – TiCl_4 – 0.018 mol, CH_4 – 0.031 mol, SiCl_4 – 0.085 mol, O_2 – 0.072 mol H_2 – 0.024 mol, 2 sample – TiCl_4 – 0.027 mol, CH_4 0.031 mol, SiCl_4 0.085 mol, $\text{O}_2=0.072$ mol, $\text{H}_2=0.024$ mol).

3. Results and discussion

The size and shape of the particles of the $\text{Si}_x\text{Ti}_y\text{C}_z\text{O}_w$ composite were examined by transmission electron microscopy using the JEOL-II-100 electron microscope (Jeol Ltd., Japan). TEM-images of the composite powders obtained by the pulsed plasma chemical method are shown in figure 2.

It can be seen from TEM photographs that the $\text{Si}_x\text{C}_y\text{O}_z$ particles have a regular shape in the form of round balls with a diameter of 50 to 200 nm. Most of the particles are covered with smaller particles of titanium oxide with an average size of 5-15 nm. The composite consists of two composition both a core of regular shape and a shell in the form of fine particles of irregular shape. It can be assumed that the core is encapsulated in titanium oxide. In the images of the particles, two areas are visible, dark and light. The dark area corresponds to a more dense TiO_2 (4.2 g/cm^3), while the light one corresponds to a less dense SiO_2 (2.7 g/cm^3).

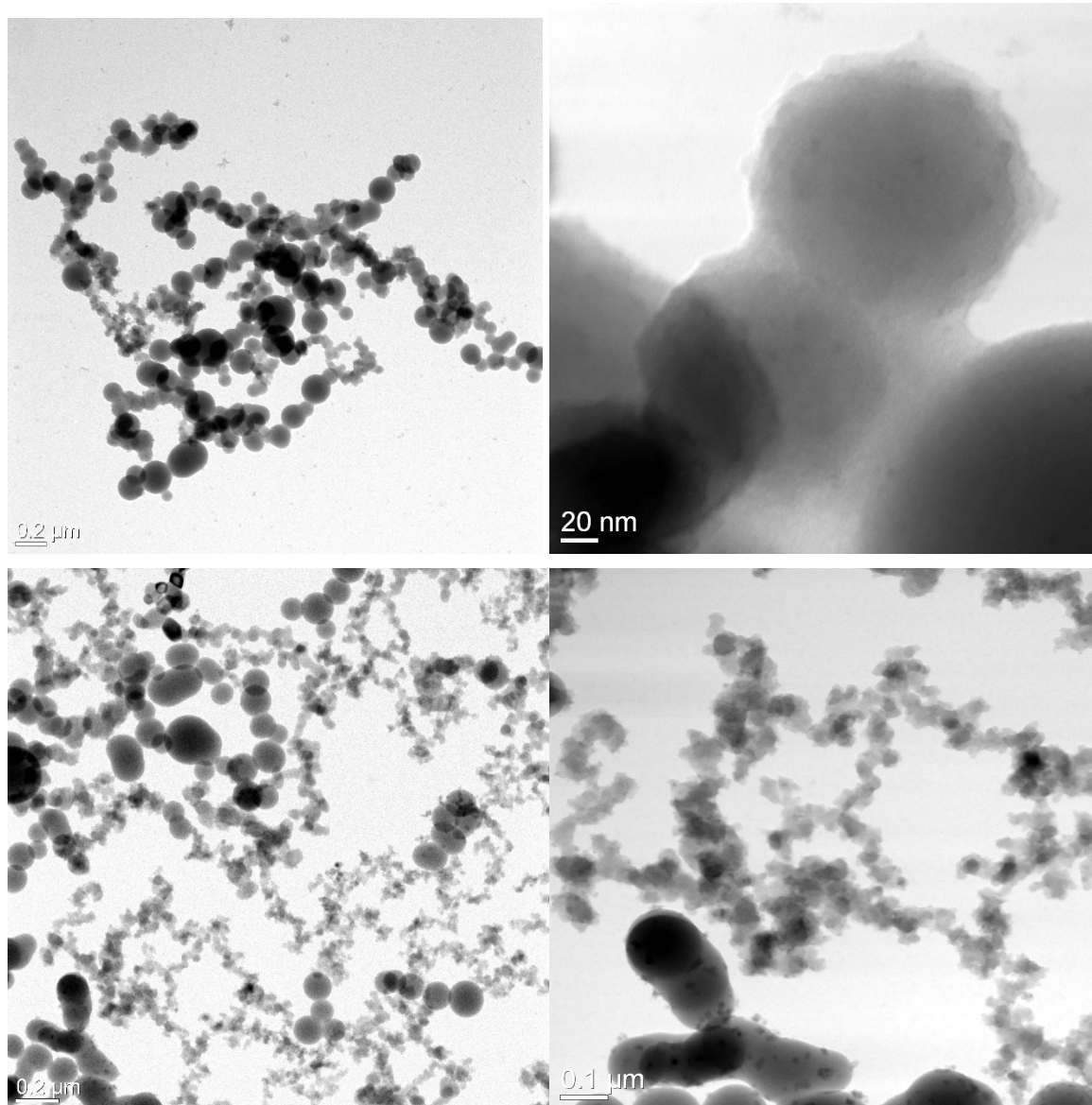


Figure 2. TEM-images of the carbon-containing composite based on silicon oxide modified with titanium oxide: sample 1 (upper photos) and sample 2 (bottom photos).

Then the spectral dependence of the absorption coefficient $\alpha(h\nu)$ was calculated from the reflection spectra according to the formula

$$\alpha(h\nu) = A \frac{(1-R(h\nu))^2}{R(h\nu)} \quad (1)$$

The value $A=1000 \text{ cm}^{-1}$ was chosen for the factor characterizing the efficiency of light scattering. The interband absorption parameters are determined in the energy intervals $\Delta'(h\nu)$ when the absorption spectra are approximated by the power law, conventional for crystalline materials:

$$\alpha(h\nu) \sim (h\nu - E_g'')^m \quad (2)$$

where $m=1/2$ and 2 correspond to direct and indirect interband allowed transitions through the optical gap for the direct E_g' and for indirect transitions E_g'' (figure 3).

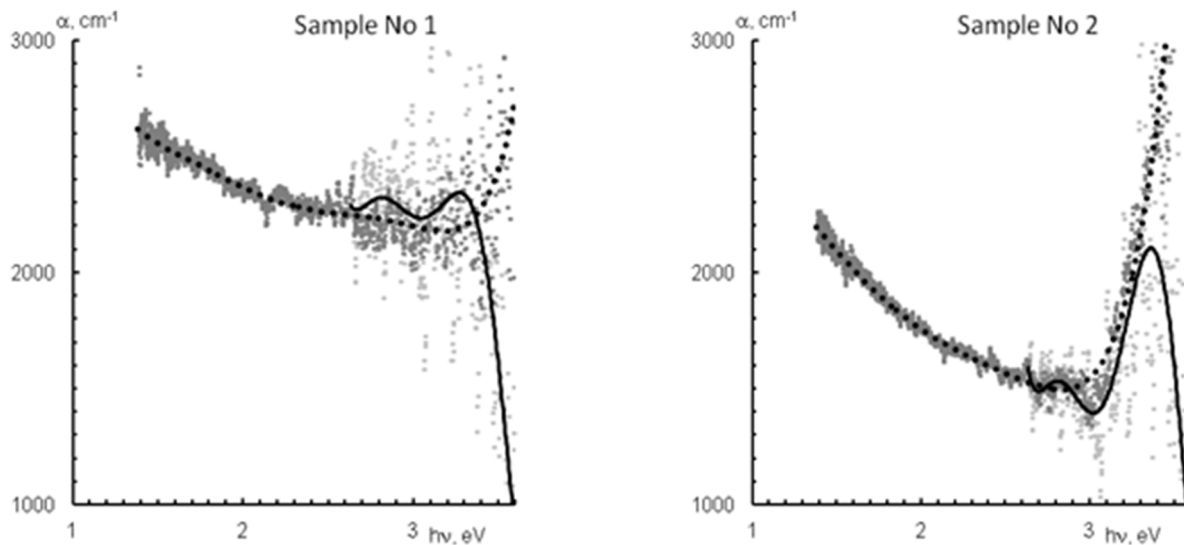


Figure 3. The interband absorption in the model developed for the absorption of amorphous semiconductors in the $\text{Si}_x\text{Ti}_y\text{C}_z\text{O}_w$ composite powder.

The width of the band gap is in the case of indirect and direct allowed transitions for sample No. 1 $E_g''=2.03 \text{ eV}$ and $E_g'=3.12 \text{ eV}$, for sample No. 2 $E_g''=2.13 \text{ eV}$ and $E_g'=2.96 \text{ eV}$, respectively. A narrowing of the band gap to $E_g''=2.03 \text{ eV}$ for indirect transitions is detected. The most likely cause of contradictory differences in the behavior of the width of the band gap is the effect on the edge of optical absorption of growth defects of unknown nature that have deep levels in the band gap with energy $h\nu \geq 3 \text{ eV}$.

4. Conclusion

The $\text{Si}_x\text{Ti}_y\text{C}_z\text{O}_w$ composite was first obtained using the pulsed plasma chemical method. Varying the concentration of the initial reagents, we can obtain the composite with different content of elements included in the composite. The morphology of the particles and the ratio of the crystal phases of the composite also depend on the initial concentration of the precursors. In the present work, the morphology of the particles is presented by the large round particles and by smaller crystallites compared to round ones. The paper presents the study of the optical properties (the spectrum of the absorption coefficient, interband absorption for the indirect transitions) of the $\text{Si}_x\text{Ti}_y\text{C}_z\text{O}_u$ composite obtained using the pulsed plasma chemical method. The band gap of the obtained composite is 2.03–3.12 eV.

Acknowledgements

This work was supported by the MES of RK grant “Pulsed plasma-chemical synthesis of new generation TiO_2 photo catalysts”.

References

- [1] Pedro G R and Hybrid 2001 *Adv. Mater.* **13** 163
- [2] Chen X and Mao S 2007 *Chem. Rev.* **107** 2891
- [3] Kojima T, Ishizu T, Horiba T and Yoshikawa 2009 *J. Power Sources* **189** 859
- [4] Matos J, Miranda C, Poon P and Mansilla H 2016 *Sol. Energy* **134** 64
- [5] Gong H, Li N and Qian Y 2013 *Int. J. Electrochem. Sci.* **8** 9811
- [6] Wu X, Shi Z, Wang C and Jin J 2015 *J. Electroanal. Chem.* **746** 62
- [7] Molkenova A and Taniguchi I 2015 *Adv. Powder Technol.* **26** 377
- [8] Furukawa S, Shishido T, Teramura K and Tanaka T 2012 *ACS Catal.* **2** 175
- [9] Yuan Y, Wang S, Kang Z and Jiao S 2015 *Electrochemistry* **83** 421
- [10] Ren Y, Wei H, Huang X and Ding J 2014 *Int. J. Electrochem. Sci.* **9** 7784
- [11] Liu P, Xie S, Peng M, Ni L, Tang Y and Chen Y 2014 *J. Sol-Gel Sci. Technol.* **73** 270
- [12] Lombardi B, Pompeo F, Scian A and Nichio N 2013 *Mater. Lett.* **106** 393
- [13] Lv P, Zhao H, Wang J, Liu X, Zhang T and Xia Q 2013 *Journal of Power Sources* **237** 291
- [14] Vital A, Richter J, Figi R, Nagel O, Aneziris C, Bernardi J and Graule T 2007 *Ind. Eng. Chem. Res.* **46** 4273
- [15] Ju T, Lee H and Kang M 2014 *J. Ind. Eng. Chem.* **20** 2636
- [16] Costa E, Zarbin A and Peralta-Zamora P 2013 *Materials Research Bulletin* **48** 581
- [17] Li H, Wanga D, Fan H, Wang P, Jiang T and Xie T 2011 *J. Colloid Interface Sci.* **354** 175
- [18] Costa E, Zamora P and Zarbin A 2012 *J. Colloid Interface Sci.* **368** 121
- [19] Egerton T, Janus M and Morawski A 2006 *Chemosphere* **63** 1203
- [20] Li M, Zhou S, Zhang Yu, Chen G and Hong Z 2008 *Appl. Surf. Sci.* **254** 3762
- [21] Zhang G, Teng F, Zhao C, Chen L, Zhang P, Wang Y, Gong C, Zhang Z and Xie E 2014 *Appl. Surf. Sci.* **311** 384
- [22] Parayil S, Kibombo H and Koodali R 2013 *Catal. Today* **199** 8
- [23] Zatil Amali Che Ramli, Nilofar Asim, WanN R W Isahak, Zeynab Emdadi, Norasikin Ahmad-Ludin, Ambar Yarmo M and Sopian K 2014 *Sci. World J.* **2014** 415136
- [24] Kabyshev A V, Konusov F V and Remnev G E 2011 *J. Surf. Invest.: X-Ray, Synchrotron Neutron Tech.* **5** 228